Géomorphologie : relief, processus, environnement, 2014, n° 2, p. 159-174

Assessment of forested shallow landslide movements coupling tree ring records from stems and exposed roots

Utilisation des racines déchaussées pour la reconstruction de l'activité passée des glissements de terrain superficiels

Jérôme Lopez Saez*, Christophe Corona**, Markus Stoffel***, Frédéric Berger*

Abstract

The purpose of this study is to explore and illustrate the potential of exposed roots to reconstruct larger-scale landslide activity and thus to complement tree-ring data gathered from stems to reconstruct spatio-temporal patterns of landslide reactivation. Work was undertaken in a forested area of the Davids-Bas landslide, Barcelonnette (Southeastern French Alps) and based on growth disturbances (GD) from 48 stems and on anatomical changes (decrease of cell lumina) in 20 exposed root sections of heavily affected Mountain pine (*Pinus uncinata* Mill. ex Mirb.) trees growing on the scarps and upon the landslide body. A total of 95 GD and 20 anatomical changes were identified in the samples pointing to 7 movements of the landslide body since AD 1977. The study demonstrates that reconstructions of landslide reactivations obtained from exposed roots samples are not significantly different from those gathered from stems, but that the inclusion of exposed roots permits realization of frequency maps in sectors which could not be documented with classic dendrogeomorphic approaches focusing on tree-ring records from stems (scars, cracks). In addition, and even more importantly, the inclusion of exposed roots allowed assessment of the geomorphic evolution of the landslide at the local scale and to detect precursor signals of major reactivations in the form of crack widening before the main movement was registered in the tree stems. In that sense, the combined approach presented in this paper can be considered as a valuable tool for land-use planners and emergency cells in charge of forecasting future events and in protecting people and their assets from the negative effects of landslides.

Key words: dendrogeomorphology, exposed root, landslide, French Alps.

Résumé

L'objectif de cette étude est de démontrer le potentiel des racines déchaussées pour la reconstitution de l'activité de glissements de terrain passés. L'étude a été réalisée sur le glissement de terrain des Davids-Bas, situé sur le versant sud du bassin de Barcelonnette (Alpes de Haute-Provence, France). L'analyse dendrogéomorphologique repose sur l'étude de 48 pins à crochets présentant des signes traumatiques caractéristiques d'une instabilité dont 11 ont fait l'objet de prélèvements additionnels au niveau du système racinaire. L'analyse des sections de racines et de tige a permis de dater 95 perturbations anatomiques depuis 1968 et de reconstruire 7 réactivations du glissement des Davids-Bas (1977, 1978, 1979, 1984, 1996, 2001 et 2004). Les racines déchaussées enregistrent des réactivations non détectées au niveau de la tige. Elles permettent donc d'affiner la cartographie des périodes de retour. D'autre part, le caractère abrupt des variations anatomiques observées révèle une exposition résultant de processus d'érosion brutaux et non d'une érosion continue. Il nous renseigne, de ce fait, sur la magnitude des réactivations passées. Enfin, l'analyse des sections racinaires prélevées au niveau des escarpements et de fissures de tension situées en amont de ces escarpements permet de reconstruire précisément l'évolution micro-topographique du versant. L'étude confirme l'apport des analyses couplées tiges/racines pour la reconstitution de la dynamique spatio-temporelle des glissements de terrain superficiels et suggère une prise en compte systématique des racines exposées dans les reconstructions futures.

Mots clés : *dendrogéomorphologie, racine déchaussée, glissement de terrain, Alpes françaises.*

Version française abrégée

Dans les Alpes, les glissements de terrain font partie des processus géomorphologiques les plus répandus et sont à l'origine de nombreux dommages socio-économiques (Hilker et al.*, 2009). La détermination des facteurs déclenchants de ces mouvements de masse et leur cartographie constituent des enjeux majeurs pour les scientifiques mais également pour les gestionnaires (Magliulo* et al.*, 2008). À l'échelle locale, des chronologies précises de l'occurrence de l'aléa et de son*

* Institut national de Recherche en Sciences et Technologies pour l'Environnement et l'Agriculture (Irstea) – UR EMGR – 38402 St-Martin-d'Hères cedex – France (jerome.lopezsaez@gmail.com).

** CNRS UMR 6042 – Geolab – 63057 Clermont-Ferrand cedex – France.

*** Dendrolab.ch – Institute of Geological Sciences – University of Bern – 3012 Bern – Switzerland.

extension spatiale constituent un prérequis indispensable à toute analyse du risque. Malheureusement, l'évolution de la fréquence de l'aléa est largement biaisée par des connaissances lacunaires de l'activité passée des glissements de terrain tant sur le plan spatial que temporel (Aleotti et Chowdhury, 1999). Sur les glissements de terrain superficiels forestiers, la dendrogéomorphologie permet de reconstruire, avec une résolution temporelle saisonnière et une emprise spatiale décamétrique, l'activité du processus, à partir de l'analyse des perturbations anatomiques contenues dans les cernes de croissance (Alestalo, 1971 ; Shroder, 1978 ; Butler and Malanson, 1985 ; Schweingruber, 1996 ; Stoffel and Bollschweiler, 2008 ; Astrade et al.*, 2012 ; Stoffel* et al.*, 2013a). En cas de survie de l'arbre à l'activité du processus, les réponses observées peuvent concerner la croissance radiale (cerne ou série de cernes anormalement étroits ou larges), sa morphologie (cicatrice, reprise de croissance apicale, changement d'axe, courbure, racine adventive) ou son anatomie (formation de bois de réaction, de rangées tangentielles de canaux résinifères traumatiques, modifications de la structure cellulaire ; Astrade* et al.*, 2012). L'activité du glissement de terrain peut également causer une exposition partielle ou totale du système racinaire. Récemment, Corona* et al. *(2011a,b) ont démontré que ce déchaussement coïncidait avec une diminution de la surface du lumen des trachéides du bois initial. Stoffel* et al. *(2013b) suggèrent, de ce fait, que les racines déchaussées peuvent constituer des indicateurs particulièrement fiables de l'activité des mouvements de masse. L'objectif de cette étude, pionnière, est de valider cette hypothèse et de démontrer l'apport de cet indicateur pour la reconstitution de l'activité de glissements de terrain passés. L'étude a été réalisée sur le glissement de terrain des Davids-Bas, situé sur le versant sud du bassin de Barcelonnette, à 2 km au sud-ouest de Jausiers (Alpes de Haute-Provence, France). Dans un premier temps, une cartographie géomorphologique des formes associées à l'activité du glissement de terrain a été réalisée. À partir de cette cartographie, 48 pins à crochets présentant des signes traumatiques caractéristiques d'une instabilité ont été échantillonnés au niveau de la tige et 11 ont fait l'objet de prélèvements additionnels au niveau du système racinaire. En laboratoire, les échantillons prélevés sur les tiges ont été analysés et les données traitées suivant les procédures standards en dendrochronologie (Stokes and Smiley, 1968 ; Bräker, 2002 ; Stoffel and Perret, 2006 ; Astrade* et al., *2012). Pour les sections racinaires, une diminution de 60 % de la surface du lumen des trachéides a été utilisée pour la détection de l'année de déchaussement (Corona* et al.*, 2011a). L'analyse des sections de racines et de tige a permis de dater 95 perturbations anatomiques depuis 1968 et de reconstruire 7 réactivations du glissement des Davids-Bas (1977, 1978, 1979, 1984, 1996, 2001 et 2004). Les racines déchaussées enregistrent des réactivations non détectées au niveau de la tige. Elles permettent donc d'affiner la cartographie des périodes de retour. D'autre part, le caractère abrupt des variations anatomiques observées révèle une exposition résultant de processus d'érosion brutaux et non d'une érosion continue. Il nous renseigne, de ce fait, sur la magnitude des réactivations passées. Enfin, l'analyse des sections racinaires prélevées au niveau des escarpements et de fissures de tension situées en amont de ces escarpements permettent de reconstruire précisément l'évolution microtopographique du versant. L'étude confirme ainsi l'apport des analyses couplées tiges/racines pour la reconstitution de la dynamique spatio-temporelle des glissements de terrain superficiels et suggère une prise en compte systématique des racines exposées dans les reconstructions futures.*

Introduction

Each year, mass movements cause considerable financial damage to alpine societies (Hilker *et al*., 2009). As a consequence, their occurrence has recently become a topic of major interest for both researchers and local administrators, especially in terms of landslide hazard and risk assessments (Magliulo *et al*., 2008). The steadily growing interest in landslides certainly reflects the increasing awareness of the socio-economic significance of the process (Aleotti and Chowdhury, 1999) but also indicates quite clearly that human pressure on the environment is becoming ever more important for land development and urbanization (Petrascheck and Kienholz, 2003). An appropriate assessment of existing and potential future landslide hazards becomes a prerequisite for a sustainable land-use, but requires, among others, a detailed determination of the spatial and temporal occurrences of landslides at the site level. However, major obstacles normally exist to obtain this kind of data, mainly due to the lack of reliable historical records on the frequency and localization of past events (Aleotti and Chowdhury, 1999). As a consequence, past research on landslides focused more on their susceptibility (see Guzzetti, 2000, and references therein for a review) rather than on the documentation of landslide hazards at the level of individual sites.

On shallow landslide bodies covered with trees, dendrogeomorphology (Alestalo, 1971; Shroder, 1978; Butler and Malanson, 1985; Schweingruber, 1996; Stoffel and Bollschweiler, 2008; Astrade *et al*., 2012; Stoffel *et al*., 2013a) has been frequently used to reconstruct landslide reactivations via the analysis of growth disturbances (GD) contained in tree-ring records. As trees suffering from superficial and slow movements may survive reactivations and thus conserve the evidence of tree topping, tilting (or S-shaped stems) and scars in their increment series (Carrara and O'Neill, 2003; Stefanini, 2004), spatial and temporal patterns of past landsliding can be dated using tree-ring samples from stem.

In landslide prone areas, tree roots resist tension, thereby increasing the shear strength of shallow soils through mechanical reinforcement (Shewbridge and Sitar, 1989; Skaugset, 1997). Partially exposed roots record the timing of past erosion pulses which can be assessed through the analysis of characteristic anatomical features in the wood of exposed roots (Gärtner *et al*., 2001; Gärtner, 2007; Corona *et al*., 2011a,b). Previous studies using increment rings in exposed roots (root rings) focused primarily on the quantification of (i) long-term aerial denudation rates (*e.g*., LaMarche, 1961; Carrara and Carroll, 1979), (ii) gullying processes (Vandekerckhove *et al*, 2001; Malik, 2008; Corona *et al*., 2011a,b; Lopez Saez *et al*., 2011; Silhan, 2012), (iii) channel wall erosion in ephemeral flash

Id	Environment	Location	Latitude	Longitude	Process	Rates	Units	References	Latitudedec	Longitudedec
1	Badlands	Spain	41°10' N	3°48' W	Sheet erosion	6.2-8.8	mm.yr-1	Bodoque et al., 2011	41,1667	-3,8
2	Badlands	France	44°08' N	6°20' E	Soil erosion	0.5	mm.yr-1	Corona et al., 2011b	44,1333	6,333
3	Badlands	Italy	43°14' N	11°33' E	Water erosion	3.75-0.27	cm.yr-1	Bollati et al., 2012	43,2333	11,55
4	Differents environments	USA	39°20' N	106°52' W	Sheet erosion	1.18	mm.yr-1	Carrara and Caroll, 1979	39,3333	-106,8667
5	Drainage basin	USA	33°37' N	111°50' W	Sediment yield	–	–	McCord, 1987	33,6167	-111,8333
6	Drift-sand areas	Netherlands	51°40' N	5°05' E	Sedimentation process	-	-	den Ouden et al., 2007	51,6667	5,0833
7	Dunes	Poland	54°41' N	17°14' E	Sedimentation process	2.4-3.5	mm.yr-1	Koprowski et al., 2010	54,6833	17,2333
8	Forest	USA	54°30 N	69°00' W	Caribou Herd	-	-	Bourdreau et al., 2003	54,5	-69
9	Gullies	France	44°08' N	6°20' E	Sheet erosion	5.9-6.2	mm.yr-1	Corona et al., 2011a	44,1333	6,333
10	Gullies	France	44°08' N	6°20' E	Sheet erosion	5.9	mm.yr-1	Lopez et al., 2011	44,1333	6,333
11	Gullies	Sapin	37°41' N	1°42' E	Headwall gully retreat	5.6	m3.yr-1	Vandekerckhove et al., 2001	37,6833	1,7
12	Gullies	Poland	50°21' N	17°51' E	Small gully retreat	0.63	m.yr-1	Malik, 2008	50,35	17,85
13	Gullies	Poland	50°04' N	14°24' E	Soil erosion	-	-	Malik, 2006	50,0667	14,4
14	Hiking trails	Spain	40°52' N	4°01 W	Sheet erosion	2.6-1.6	mm.yr-1	Bodoque et al., 2005	40,8667	-4,01667
15	Hiking trails	Italy	46°24' N	10°31' E	Soil erosion	2.7	mm.yr-1	Pelfini and Santilli, 2006	46,4	10,51667
16	Hiking trails, anatomical response	-	40°59' N	4°05' E	Sheet erosion	-	-	Rubiales et al., 2008	41,3167	4,0833
17	Hillslopes	USA	37°37' N	118°22 W	Sheet erosion	0.015-0.12	mm.yr-1	Lamarche, 1961, 1963, 1968	37,6167	-118,3667
18	Hillslopes	USA	36°09' N	109°33' W	Sheet erosion	1.9	mm.yr-1	Mc Auliffe et al., 2006	36,15	-109,55
19	Karst area, anatomical response	China	14°26' N	105°42' E	Soil erosion		-	Luo et al., 2011	14,4333	105,7
20	Lakes	Canada	46°35' N	72°01' W	Shore erosion	0.15	m3.m-2.yr-1	Bégin et al., 1991	46,5833	-72,0167
21	Lakes	USA	32°23' N	110°42' W	Shore erosion	1	mm.yr-1	Danzer, 1994	32,3833	-110,7
22	Methodological				Soil erosion	-	-	Gärtner, 2007		
23	Methodological				Soil erosion	-	-	Ballesteros et al., 2012		
24	Pine forest	Spain	40°12 N	3°34' W	Sheet erosion	3.5-8.8	mm.yr-1	Pérez-Rodriguez et al., 2007	40,2	-3,5667
25	Rangelands	Kenya	1°26' S	36°57' E	Soil erosion	5.5	mm.yr-1	Dunne et al., 1978	-1,4333	36,95
26	Rangelands	Patagonia	42°58' S	64°20' W	Soil erosion	2.4-3.1	mm.yr-1	Chartier et al., 2009	-42,9667	-64,3333
27	Riverbank	Czech Republic	50°15' N	15°05' E	Bank erosion	-	-	Malik and Matyja, 2008	50,25	15,0833
28	Riverbank	Switzerland and Germany	46°17' N	7°32' E	Water erosion	-	-	Gartner et al., 2001	46,2833	7,5333
29	Riverbank	Patagonia	40°56' S	71°24' W	Bank erosion	-	-	Stoffel et al., 2012	-40,9333	-71,4
30	Riverbank, anatomical response	Switzerland	47°00' N	8°31' E	Water erosion	-	-	Hitz et al., 2008a,b	47	8,5167
31	Sea	Italy	42°36' N	11°57' E	Shore erosion	0.028-0.092	m.yr-1	Fantucci, 2007	42,6	11,95

Tab. 1 – **Overview of work published on dendrogeomorphic reconstruction based on analysis of exposed roots.**

*Tab. 1 – **Synthèse bibliographique des reconstructions dendrogéomorphologiques réalisées à partir de l'analyse des racines déchaussées.***

flood channels (Stoffel *et al*., 2012) and on (iv) shore erosion (Bégin *et al*, 1991; Fantucci, 2007; Rovéra *et al*., 2013; tab. 1). In their recent review paper, Stoffel *et al*. (2013b) suggested that the sudden opening of cracks in landslide bodies would represent yet another field where exposed roots could be used to assess initial crack opening as well as widening rates.

In line with these proposals, this study aims at (i) exploring and illustrating the potential of living roots spanning cracks in active landslide bodies to record reactivations and at (ii) assessing their potential to complement data obtained with classical dendrogeomorphic data obtained from stems of disturbed trees growing on the landslide body itself.

Study site

The Davids-Bas landslide (DB; 44°24'19''N, 6°43'34''E; fig. 1A) is located on the S-facing slope of the Barcelonnette basin, 2 km SW of Jausiers (Alpes de Haute-Provence, France). The landslide body is 175 m long, 200 m wide, and ranges from 1250 to 1200 m a.s.l. in elevation; it is characterized by an irregular topography with slope gradients ranging from 9° to 33°. The DB landslide body is partially covered by Mountain pines (*Pinus uncinata* Mill. ex Mirb.) and grasslands (Lopez Saez, 2011; fig. 1A).

Bedrock consists of Callovo-Oxfordian black marls in the lower part and Eocene flyschs further upslope (Lopez Saez, 2011). Both units are covered with a 1- to 5-m thick ground moraine deposit, thereby rendering the area even more vulnerable to mass-movement activity. Under dry conditions, black marls are relatively stable and can absorb large quantities of water, but they soften considerably when wet (Antoine, 1995).

Climate at DB is reflective of dry and mountainous Mediterranean environments and shows strong interannual rainfall variability. Precipitation at Barcelonnette (44°38' N, 6°65' E) is 707 mm/yr for the period 1928–2010. Rainfall can be violent, with intensities > 50 mm/h, especially during frequent summer storms. Melting of the snow cover, which usually persists from December to March, often adds to the saturation and runoff effect of heavy spring rainfalls (Flageollet, 1999). Mean annual temperature is 7.5°C and freezing typically occurs during 130 d/yr.

These predisposing geomorphic and climatic factors explain the occurrence of a landslide which usually affects the uppermost 2–6 m of the top moraine layer (Thiery *et al*., 2007). The DB landslide is characterized by (i) shallow rotational slides in the upper parts (fig. 1C), as well as by (ii) shallow translational earthslides and (iii) by undercutting from the lateral erosion of the left Ubaye riverbank in the lower parts of the slope (fig. 1D).

Landslides represent a major hazard in the Barcelonnette basin where the combination of predisposing factors (*i.e*., lithology, surface deposits, climate and land use) creates

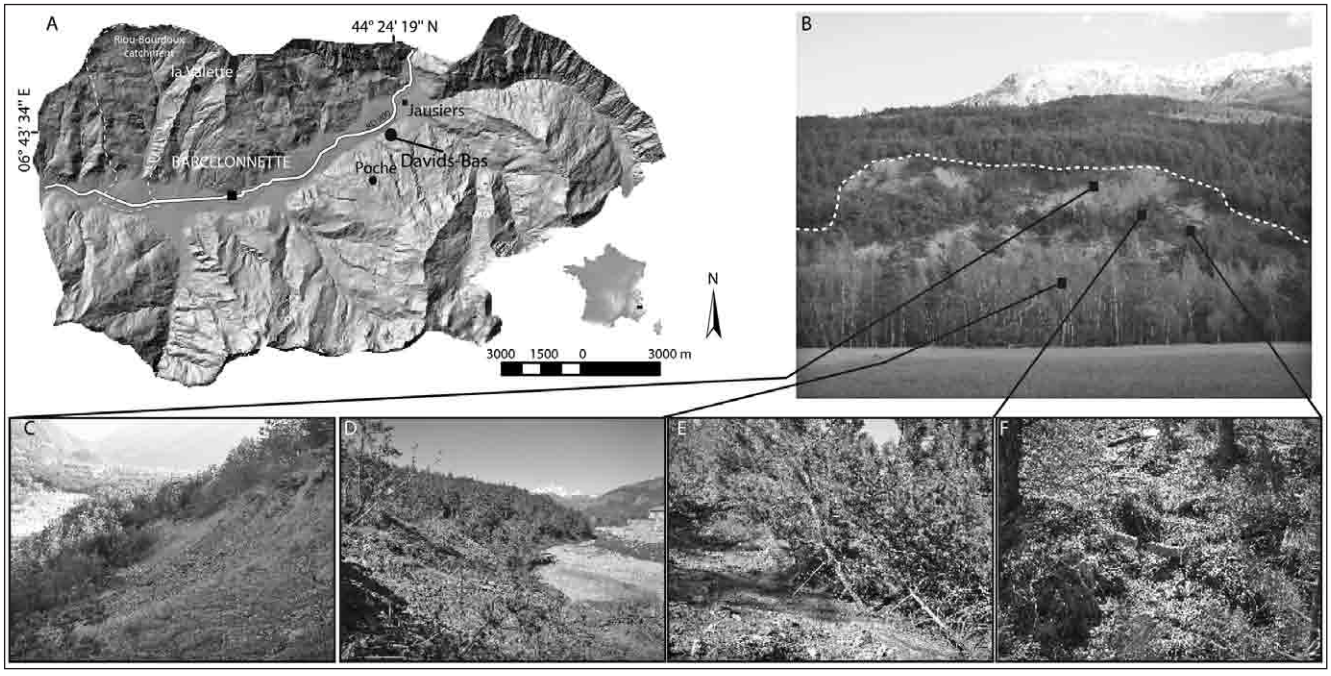

Fig. 1 – **Location and geomorphological setting of the study site.** A: the Davids Bas landslide (DB) is located in the Southern French Alps, in the Ubaye valley, near the village of Jausiers. B: view of the main scarp (SC1, dotted line) and of the landslide body. C: DB is characterized by shallow rotational slides in its upper part. D: presence of shallow translational earthslides in its lower parts undercut by Ubaye river. E: tilted trees. F: exposed roots used for the reconstruction of past landslide activity.

*Fig. 1 – **Localisation et contexte géomorphologique du site d'étude.** A : le glissement de terrain des Davids-Bas (DB) est localisé dans le Sud-Est de la France, dans la vallée de l'Ubaye, à proximité de la commune de Jausiers (Alpes de Haute-Provence). B : vue de l'escarpement principal (SC1, pointillés) et du corps du glissement. C : présence en amont, d'un escarpement principal, à composante rotationnelle. D : la base du bourrelet frontal du glissement est sapée, à l'aval, par l'Ubaye. E : formation de bois de compression suite à un basculement. F : exposition partielle du système racinaire.*

favourable conditions for the triggering of mass movements (Lopez Saez, 2011). Archives yield information on more than 150 landslide events in the Barcelonnette basin since AD 1850 (Amiot and Nexon, 1995; Flageollet, 1999). Yet, for the DB landslide, no event has been inventoried in the regional database (Lopez Saez, 2011). This lack of records is partly due to the fact that (i) the DB landslide is not putting life or property at risk; (ii) the Barcelonnette basin has a relatively low population density, resulting in many slope failures remaining unnoticed; and (iii) the attention largely focuses on the extremely active and large landslides causing a high potential risk (such as the La Valette, Super-Sauze and Poche landslides (fig. 1A). However, the presence of buried and tilted trees (fig. 1E) with exposed roots (fig. 1F) on scarps and open cracks clearly indicates that there are reasons to believe that this site has produced multiple landslide reactivations in the past and that it has the potential to inform about the value of exposed root analysis to conventional tree-ring records obtained from stem samples.

Material and methods

Geomorphic mapping and sampling strategy

As a first step, geomorphic mapping of landforms associated with past landslide activity was realized in a scale of 1:1000, before the position of disturbed trees was obtained with an accuracy < 1 m using a Trimble GeoExplorer GPS. Thereafter, 192 increment cores were sampled from 48 *P. uncinata* trees with obvious signs of disturbance induced by past landslides. Within this study, we preferably selected tilted and buried trees from which four cores each were extracted: two in the supposed direction of landslide movement (*i.e.,* upslope and downslope cores), and two perpendicular to the slope. To gather a maximum of information on GD caused by past events, increment cores were preferably sampled at the height of the visible damage or within the segment of the stem tilted during past events.

In addition, 20 root discs were taken from 11 previously sampled *P. uncinata*. Discs were taken at a distance > 50 cm from the stem to avoid possible mechanical effects on increment growth. Before cutting, the position of exposed roots was documented in detail and data recorded on topography, altitude, aspect, root distance from tree trunk, hillside slope, and slope of the specific root location. Exposed root samples were then cut with a handsaw into cross-sections about 2 cm thick.

Additional data gathered for each tree sampled included (i) a determination of its 3D position within the deposits; (ii) sketches and position of visible defects in the tree morphology, such as scars, buried, tilted stems and exposed roots; (iii) the position of cores sampled (*i.e.* upslope, downslope, other); (iv) tree diameter at breast height (DBH) derived from circumference measurements and (v) data on neighbouring trees as well as micro-topography (see Stoffel *et al.*, 2005, for details).

A total of 20 undisturbed trees located above the landslide scarps and showing no signs of landslide activity or other geomorphic processes were sampled to establish a reference chronology. Two cores per trees were extracted, parallel to the slope direction and systematically at breast height. This reference chronology represents common growth variations in the area (Cook and Kairiukstis, 1990) and enables precise cross-dating and age correction of the cores sampled on the landslide body.

Analysis of stem sections

The increment samples extracted from the stems were prepared, analysed and data processed following standard dendrochronological procedures (Stokes and Smiley, 1968; Bräker, 2002; Stoffel and Perret, 2006; Astrade *et al.*, 2012). Landslide movement (fig. 2) may induce several types of GD in the stem, most commonly in the form of (i) compression wood (CW, fig. 2A) on the tilted side of the stem, (ii) chaotic callus tissue resulting from the mechanical impact of debris (fig. 2B; Stoffel *et al.*, 2010) and/or abrupt reductions in annual ring width (fig. 2C; Lopez Saez *et al.*, 2012a,b). A concentric reduction in annual ring width over several years (fig. 2) is interpreted to reflect damage to the root system, loss of a major limb, or partial burial of the trunk due to landslide movements (Van Den Eeckhaut *et al.*, 2009; Carrara and O'Neill, 2003). In this study, growth-ring series had to exhibit (i) a marked reduction in annual ring width during at least five consecutive years such that the (ii) width of the first narrow ring was 50% or less of the width of the annual ring of the previous year (Lopez Saez *et al.*, 2012a). Such sharp and long reductions are not observed in the reference chronology.

The onset of CW is interpreted as a response to stem tilting induced by pressure on the tree from the landslide material. Tilted trees try to recover straight geotropic growth (Mattheck, 1993) leading to the development of S-shaped morphologies along the trunk. In the tree-ring series, tilting of a conifer trunk results in asymmetric tree-ring growth (fig. 2A), *i.e.* in the formation of wide annual rings with smaller, reddish yellow-colored cells with thicker cell walls (so-called CW; Timell, 1986) on the tilted side and narrower (or even discontinuous) annual rings on the opposite side of the tree (Panshin and de Zeeuw, 1970; Carrara and O'Neill, 2003).

Analysis of exposed root sections

The 20 exposed root sections were first prepared for macroscopic analysis following the procedure described by Bodoque *et al.* (2005). Field sampling campaign was carried out in spring 2011. As only living exposed roots were sampled, the last growth ring though corresponded to the last growing season (2010) before sampling took place. Dating accuracy was improved by cross-counting growth rings on four different radii per section to minimize the risk of misdating through the presence of false, wedging or missing rings.

On eroding slopes, roots are likely to be affected by changes and ultimately the loss of edaphic cover which will in turn cause variations in temperature and humidity as well as a reduction of soil cover pressure (Gärtner *et al.*, 2001;

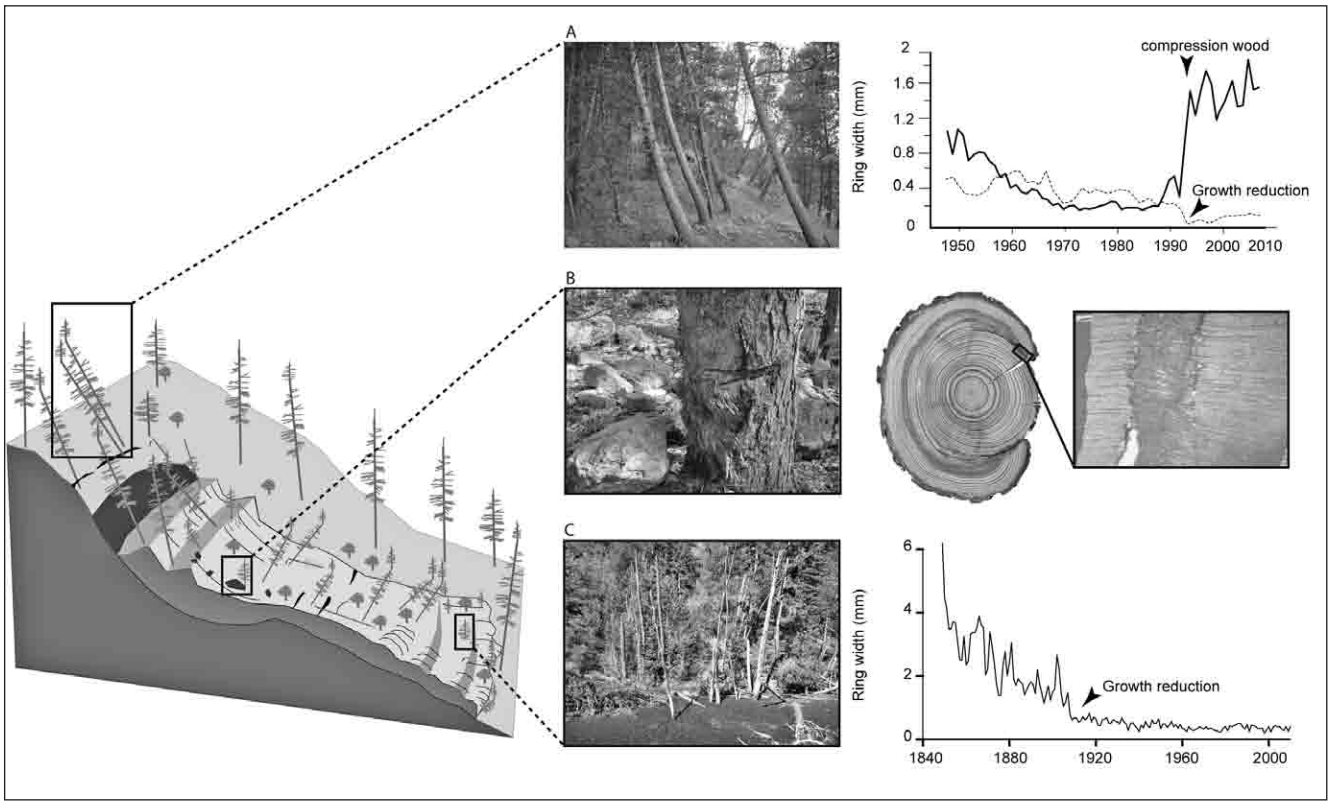

Fig. 2 – **Main dendrogeomorphic process event responses resulting from landslide activity (A, B, C). Evidence used to infer landslide events from growth anomalies in the tree ring record.**

Fig. 2 – ***Principales perturbations de croissance observées sur un glissement de terrain (A,B,C). Perturbations de croissance utilisées pour la reconstruction de l'activité passée des glissements de terrain.***

Gärtner, 2007; Corona *et al*., 2011a,b). Such changes in temperature and moisture may give rise to the formation of ice crystals in sap, air bubbles in xylem conduits and gas-filled conduits, which may ultimately impede water transport (Zimmermann, 1983) and to that effect results in cell embolism and subsequent xylem dysfunction (Arbellay *et al*., 2012). To minimize their vulnerability to freezing and embolism, the size of earlywood tracheids in *Pinus sylvestris* stems has been reported to depend on air temperature and moisture at the start of the growing season (Antonova and Stasova, 1993), with smaller cells being typically formed during periods of unfavourable conditions. Recent research realized at the Draix experimental basin has demonstrated that similar reductions in cell lumina can be observed in exposed roots of *P. sylvestris* as a result of reduced edaphic cover and the related amplification of fluctuations of temperature and humidity (Corona *et al*., 2011a,b), and that these changes can be used to accurately date root exposure.

The detection of these reductions requires microscopic analyses. Exposed root sections were recorded with a digital imaging system under optical microscopy (fig. 3) and pictures analysed using the semi-automated WinCell 2009a software to quantitatively assess changes in anatomical parameters such as the cell size distribution of earlywood tracheids. Following Rubiales *et al*. (2008) and Corona *et al*. (2011a,b), anatomical changes (AC) in tracheid cell size were determined by randomly measuring the cell lumen area of 12 tracheids per growth ring. The years of root exposure were determined by a peculiar reduction of about 60% of the lumen area of earlywood tracheids (Corona *et al*., 2011a,b).

Age structure of the stand

The age structure of the forest stand at DB was approximated by counting the number of tree rings of sampled trees and visualized after an "inverse distance weighted" interpolation using ArcGIS 9.3. Interpolations were performed using an ellipse-shaped search including data from 10 to 15 neighbouring weighted points within each of its four sectors. The same method has been used for the illustration of return period. However, since trees were not sampled at their stem base and the piths as well as the innermost rings of some trees were rotten, the age structure is biased and does neither reflect inception nor germination dates. Nonetheless, it provides valuable insights into major disturbance events at the study site with reasonable precision.

Dating of events

Determination of events was based both on the number of samples showing GD and AC in the same year and on the spatial distribution of affected roots and stems (Bollschweiler *et al*., 2008). To avoid overestimation of AC and GD

Fig. 3 – **Anatomical changes in a Pinus uncinata root from the DB landslide following sudden exposure demarcated with the dashed line.** Rings formed prior to exposure are much smaller and have larger tracheids with thinner cell walls, whereas the size of tracheids is strongly reduced (but with thicker walls) after the moment of exposure.

*Fig. 3 – **Modifications anatomiques observées sur une racine de Pinus uncinata suite à une mise à l'air brutale.** Les cernes de croissance formés avant la mise à l'air présentent des trachéides de grande taille avec une paroi mince. Les cernes postérieurs à la mise à l'air sont caractérisés par des trachéides de surface réduite, à paroi cellulaire épaisse.*

within the tree-ring series in more recent years because of the larger sample of trees available for analysis, we used an index value *(It)* as defined by Shroder (1978) and Butler and Malanson (1985):

$$It = \left(\sum_{i=1}^{n} (Rt) / \sum_{i=1}^{n} (At) \right) * 100 \quad (1)$$

Where R is the number of trees showing a GD and AC , thought to be a response to a landslide event in year t, and A is the total number of sampled trees alive in year t. It is also obvious that a tree recovering from an initial landslide event and forming very narrow annual rings or compression wood will not necessarily develop a signal after a subsequent reactivation that is different enough for it to be clearly distinguishable from the first event (Carrara and O'Neill, 2003); for this reason, significance was only assigned to the initial year of a marked reduction in annual ring width or a CW series and it was adjusted to only take account of trees with a significant record for year t (Carrara and O'Neill, 2003).

In this study, we used a threshold of $GD+AC \geq 4$ and an $It \geq 5\%$ to date simultaneous landslide reactivations within the same area of the landslide body (Lopez Saez *et al*., 2012a). These thresholds aimed at (i) minimizing the risk that GD/AC caused by other factors (possible influence of felling activity, CW induced by snow-creep) could mistakenly be attributed to a landslide event; (ii) avoiding an overestimation of response percentage resulting from a low number of trees early in the record (Dubé *et al*., 2004).

Calculation of landslide return periods

Traditionally, the return period designates the mean time interval at which a material reaches a given point in an avalanche path (McClung and Schaerer, 1993; Corona *et al*., 2010), with frequency being usually expressed as "return period" in years (*i.e*. 1/frequency). We adapted this approach and, by analogy, calculated individual tree return periods (Rp) for the DB landslide from the GD and AC frequency (in stems and exposed roots) f for each tree T following the approach presented by, *e.g*., Reardon *et al*. (2008) and Lopez Saez *et al*. (2012a,b):

$$f_T = \left(\sum_{i=T}^{n} (GD + AC) \right) \div \left(\sum_{i=T}^{n} A \right) \quad (2)$$

where $GD+AC$ represents the number of growth disturbances and anatomical changes detected in the samples taken from stems and exposed roots of tree T, and A the total

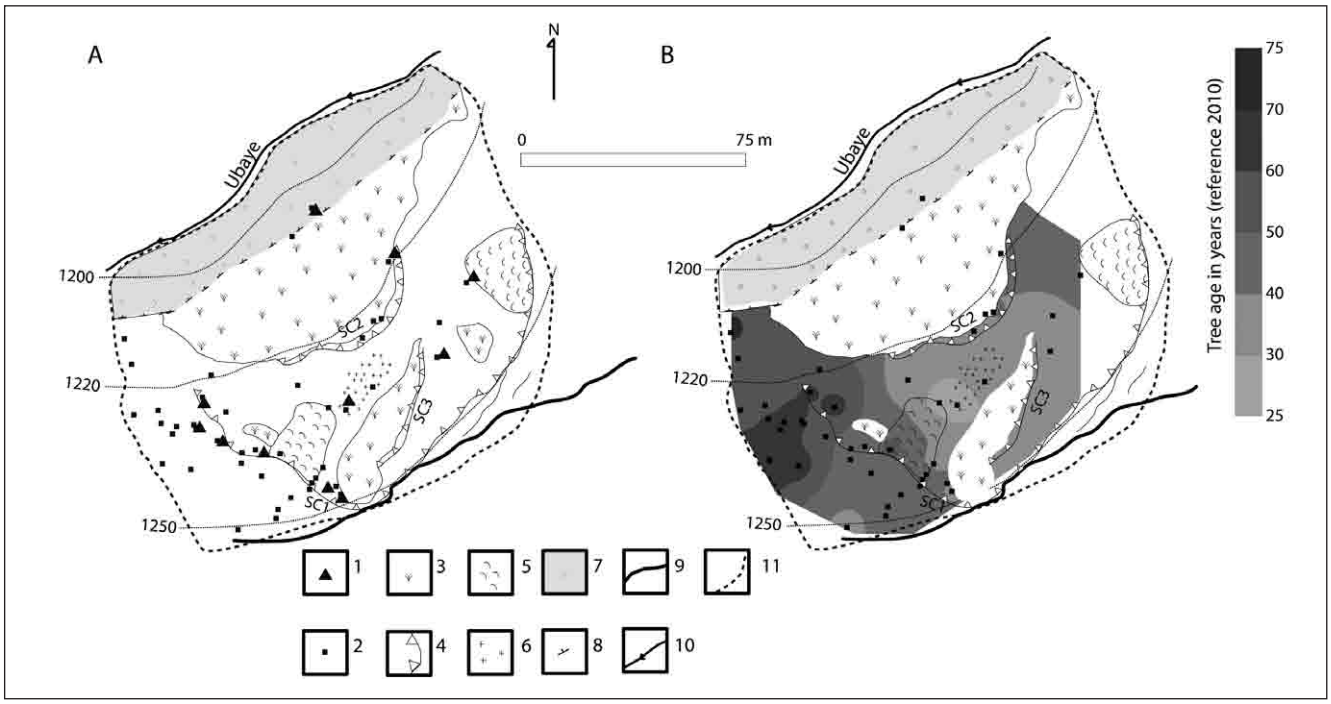

Fig. 4 – **Location of root and stem samples (A) and mean age of the 48 Pinus uncinata trees (B).** 1: exposed root sampled; 2: stem sampled; 3: open grassland; 4: main scarps; 5: earthflow; 6: bench; 7: ubaye river bank; 8: talus; 9: forest road; 10: main channel of Ubaye river; 11: limits of the DB landslide area.

Fig. 4 – ***Localisation des 48 Pinus uncinata échantillonnés (racines/tiges) (A) et cartographie de l'âge des arbres échantillonnés (B).*** *1 : localisation des racines déchaussées échantillonnées ; 2 : localisation des arbres échantillonnés ; 3 : îlot herbacé ; 4 : escarpement principal ; 5 : coulée récente ; 6 : replat topographique; 7 : dépôt torrentiel de l'Ubaye ; 8 : rupture de pente ; 9 : piste forestière; 10 : Ubaye ; 11 : limite du glissement de terrain des Davids-Bas.*

number of years where tree *T* was alive. The DB landslide return periods were visualized after an inverse distance weighted interpolation using ArcGIS 9.3. Interpolations were performed using an ellipse-shaped search including data from ten to fifteen neighbouring weighted points.

Results

Age structure of the stand and growth disturbances

Pith age data from 48 *P. uncinata* trees sampled at DB suggest (fig. 4A) an average age of the forest stand of 46±13 yr. Only 15% of the trees are older than 60 yr. As can be seen in figure 4B, the distribution of tree ages is characterized by two dominant age classes comprised between 25–40 and 40–75 yr: (i) older trees (> 40 yr) are restricted to a large patch in the westernmost portion of the landslide body (1220 m a.s.l.) whereas (ii) trees aged 25-40 yr basically cover the landslide body itself. The oldest tree exposed roots at DB shows 43 rings, whereas 20 growth rings were counted in the youngest exposed root section.

A total of 95 GD related to past landslide displacement events was identified in increment cores sampled from 48 *P. uncinata* trees. The most common reaction to movements was in the form of compression wood (76% of all GD). Abrupt growth reductions account for 24% of the reactions. The earliest GD was recorded in 1968; however, a landslide reactivation was not inferred for this year as GD were restricted to only one tree. The years 1996 (n = 20), 2001 (n = 20), 1984 (n = 10), and 1978 (n = 9) exhibit the largest number of trees with GD (fig. 5).

Abrupt decreases in cell lumen area of earlywood tracheids were observed in all exposed root sections. Inclusion of AC allowed addition of 20 ACs to the stem-based GD chronology. In the root-based chronology, the years 2001 (n = 8), 1984 (n = 5), and 1996 (n = 4) exhibit the largest number of reactions (fig. 5B). In combination, the GD and AC table yields 7 years (1977, 1978, 1979, 1984, 1996, 2001, and 2004) where the $It > 5\%$ (fig. 5A) and GD ≥ 4 trees threshold was exceeded (fig. 5B) between 1977 and 2004.

At the tree scale, the evolution of cell responses in exposed roots and in the main stem are exemplified in figure 6. Most interestingly, the reactions in exposed roots (AC) are not necessarily synchronous with those observed in the stem (GD) of the same tree, but ACs detected in the exposed roots (except 2007) correspond to one of the landslide reactivations presented just above. Conversely, no AC was observed in 1979.

Spatial distribution of trees disturbed by landslide movements

The spatial distribution of trees that have been affected by the same movement of the landslide is provided in figure 7

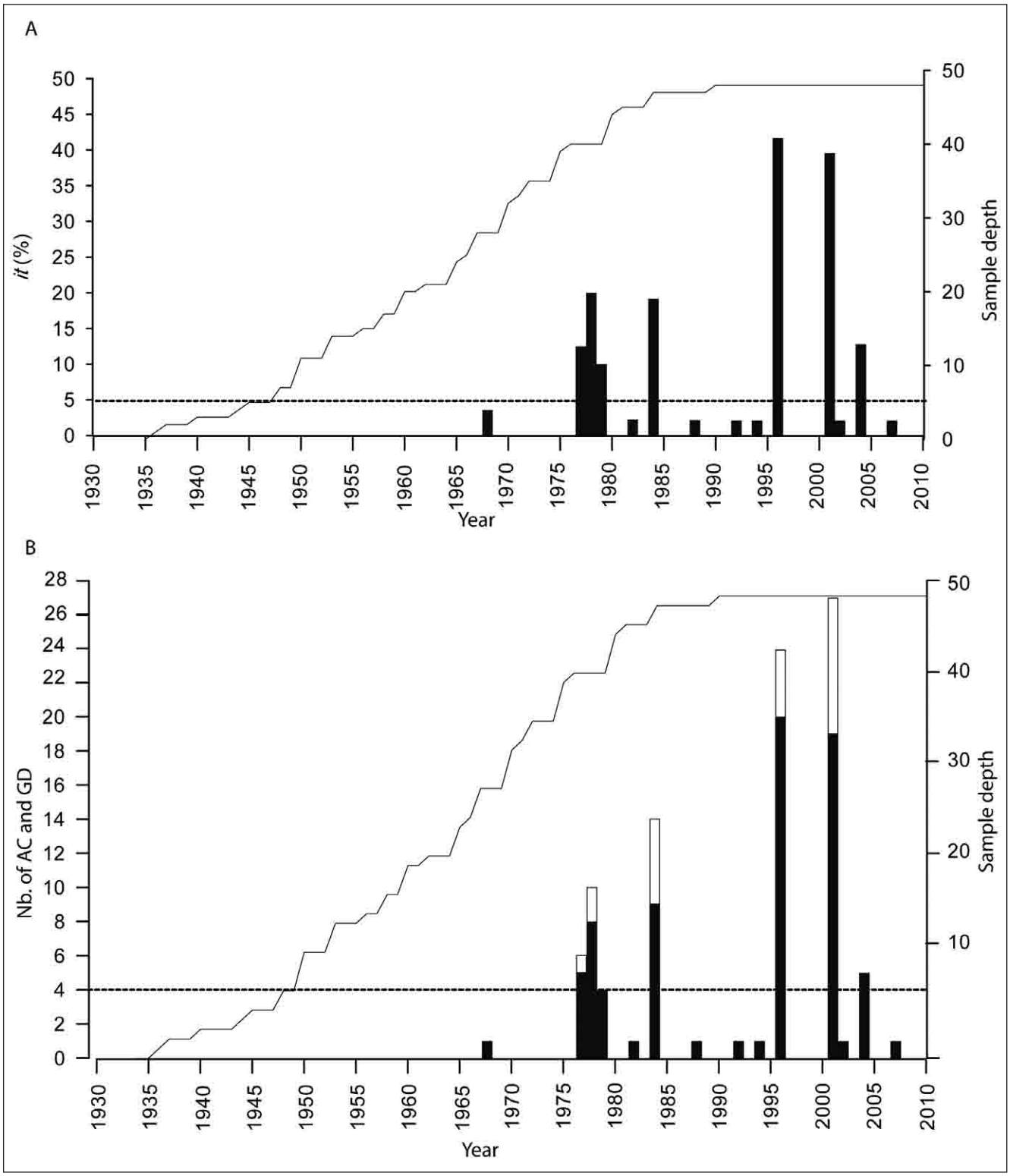

Fig. 5 – **Event response histograms showing landslide induced growth disturbances (GD, black bars) and anatomical changes (AC, white bars) from sampled trees.** A: percentage of trees (exposed roots and stems). B: total number of trees (exposed roots and stems) responding to a damaging event. The black horizontal dotted line demarcates the 5% sample depth thresholds in (A), and the n=4 tree thresholds in (B). The black line shows the sample depth (i.e. the total number of trees alive in each year). A total of 7 events could be reconstructed from the tree-ring and root-ring series since AD 1977.

*Fig. 5 – **Histogramme représentant la répartition annuelle des perturbations de croissance observées dans les tiges (GD) et des modifications anatomiques observées dans les sections racinaires (AC) échantillonnées.** A : pourcentage des arbres présentant des perturbations anatomiques dans la tige et/ou les racines. B : nombre total d'arbres présentant des perturbations anatomiques dans la tige et/ou les racines. La ligne noire horizontale représentent les seuils utilisés pour déterminer les événements : 5% des arbres vivants (A) et 4 perturbations (B). En se basant sur ces histogrammes et sur ces seuils, 7 événements ont pu être reconstruits depuis 1977.*

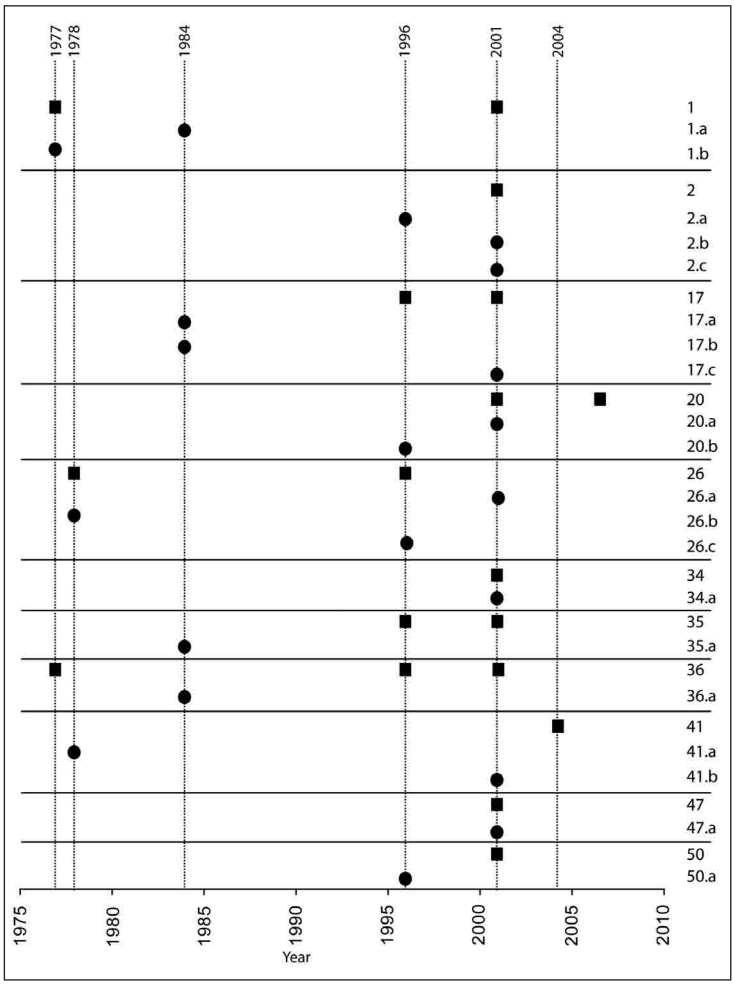

Fig. 6 – **GD and AC dated in 11 trees sampled in both stems and roots.** Squares represent the year for GD and dots the year for AC.

*Fig. 6 – **Perturbations de croissance (GD) et modifications anatomiques (AC) datées dans les 11 arbres ayant fait l'objet de prélèvement dans la tige et au niveau des racines.** Les carrés représentent les perturbations de croissance observées dans la tige, les ronds les modifications anatomiques racinaires.*

and proves to be of considerable help for the determination of the spatial extent of past reactivation events. Two general patterns of landslide reactivations can be observed at DB. In 1996 and 2001, landslide reactivations affected trees throughout the study area and therefore clearly represent major events. The analysis of AC allowed the detection of significant movements at the landslide scarps, especially on the main scarp (SC1 and associated tension cracks; fig. 4), where a majority of exposed roots sampled exhibits a strong decrease in cell lumen area during these two particular years. In 1977, 1978, 1979, 1984 and 2004, GD were more restricted to specific and rather isolated segments of the landslide body. During the reactivations of 1979 and 2004, only trees located in the eastern segment of the landslide body and below SC1 have been affected, whereas exposed roots did not show any AC during these years. In 1977, 1978 and 1984, in contrast, AC observed in exposed roots allowed delineation of the events. The information contained in the exposed root samples also supports the idea that movements occurred all along SC1 in 1984 and in cracks upslope of the somewhat minor scarp SC3 in 1978.

Trees (ID)	Individual return period computed from GD (in years)	Individual return period computed from GD+AC (in years)
1	19	12.6
2	40	20
17	22.5	15
20	26	17.3
26	30	20
34	34	34
35	13	8.6
36	17.3	13
41	20	10
47	30	30
50	60	30

Tab. 2 – **Individual return period in years computed from growth disturbances (GD) observed in the stem, individual return period in years computed from growth disturbances (GD) observed in the stem and from anatomical changes observed in root ring (GD+AC**).

*Tab. 2 – **Période de retour individuelle calculée à partir des perturbations de croissance observées dans la tige (GD), des perturbations de croissance observées dans la tige et des modifications anatomiques datées dans les sections racinaires (AC+GD).***

Return period of landslide movements

Return periods at the tree level were computed using (i) only GD as well as (ii) using GD and AC information (tab. 2). Significant decreases in return periods are observed in 9 out of 11 trees as soon as AC are included in the analysis. By way of example, return periods were reduced by 50% in trees 2 (40 to 20 event/yr), 41 (20 to 10 event/yr) and 50 (60 to 30 event/yr). Within the area sampled, return periods range from 20 to 70 yr in the maps computed with GD

Fig. 7 – **Event-response maps showing the DB landslide for each of the reconstructed reactivation events.** Large dots indicate trees disturbed by the mass movement; small dots represent trees that are alive but not affected by the reactivation. 1: tree disturbed; 2: root disturbed; 3: open grassland; 4: earthflow; 5: Ubaye river bank; 6: forest road; 7: limits of the DB landslide area; 8: living tree unaffected; 9: main scarps; 10: bench; 11: talus; 12: main channel of Ubaye river.

*Fig. 7 – **Cartes des événements reconstruits à partir de l'approche dendrogéomorphologique.** Les gros points représentent les arbres perturbés par le glissement ; les petits points représentent les arbres vivants non affectés par l'événement. 1 : perturbation observée dans la tige ; 2 : modification anatomique observée dans la racine ; 3 : îlot herbacé ; 4 : coulée récente ; 5 : dépôt torrentiel de l'Ubaye ; 6 : piste forestière ; 7 : limite du glissement de terrain des Davids-Bas ; 8 : arbre vivant non affecté par l'événement ; 9 : escarpement principal ; 10 : replat topographique ; 11 : rupture de pente ; 12 : Ubaye.*

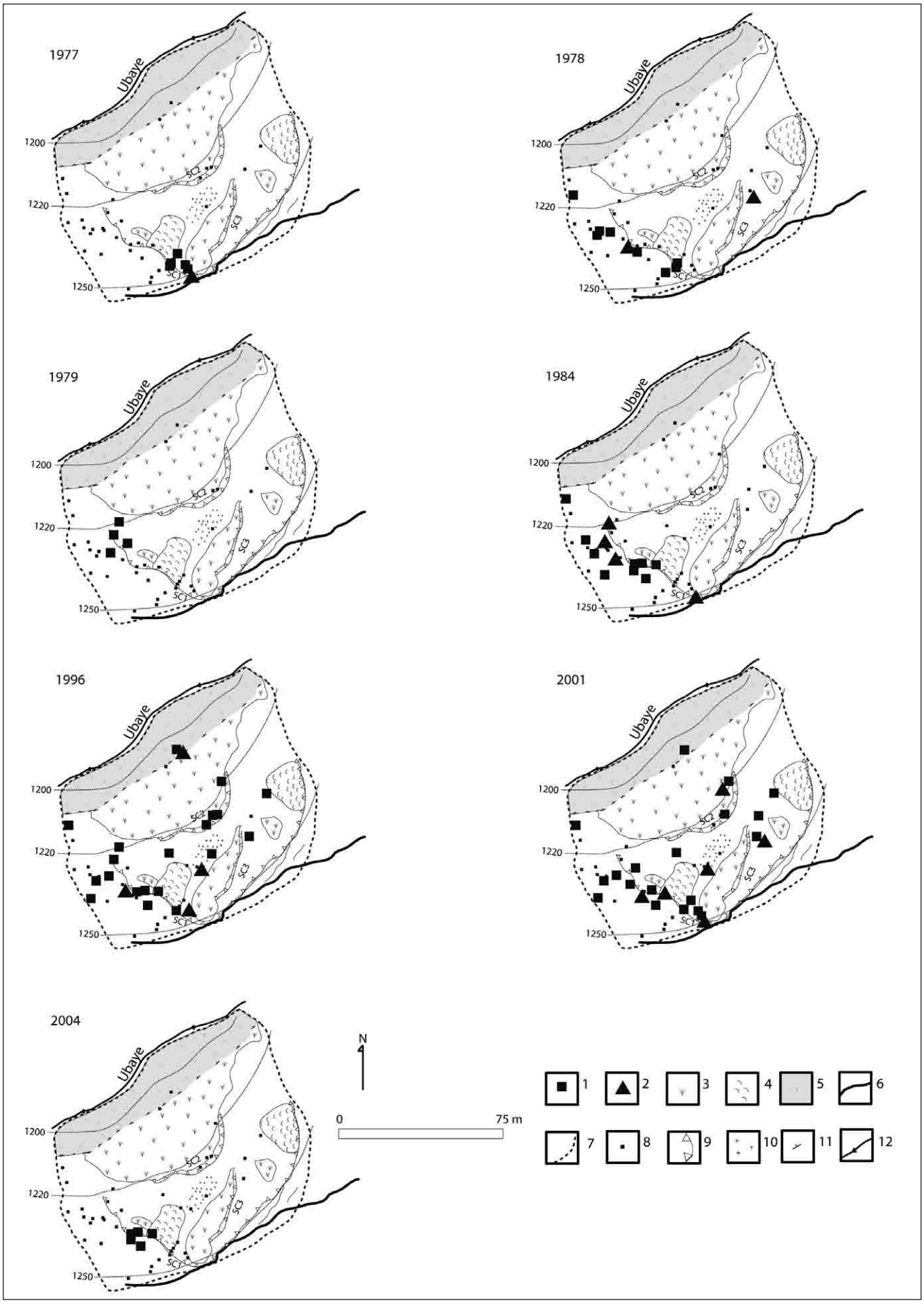
1977
1978
1979
1984
1996
2001
2004
Ubaye
1200
1220
1250
SC1
SC2
SC3
N
0
75 m
1
2
3
4
5
6
7
8
9
10
11
12

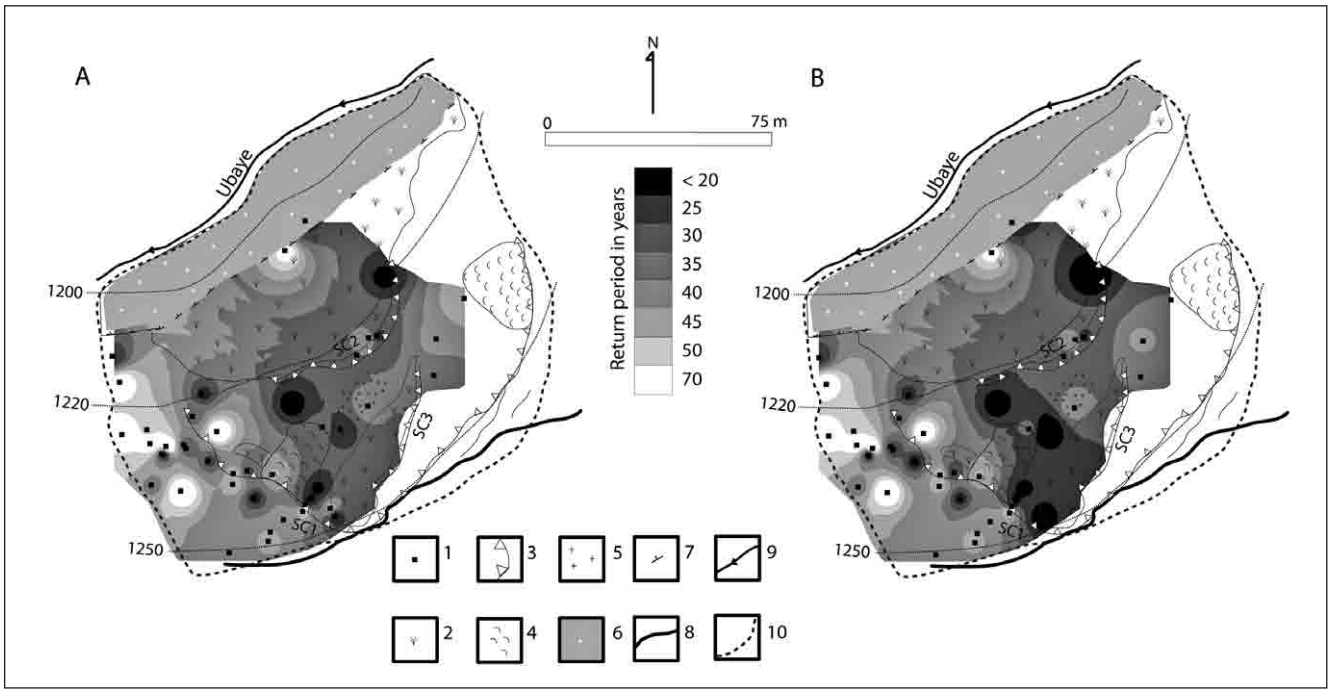

Fig. 8 – **Interpolated return periods for the sampled area of the DB landslide computed from GD (A) and GD+AC (B).** 1: sampled tree; 2: open grassland; 3: main scarp; 4: earthflow; 5: bench; 6: Ubaye river bank; 7: talus; 8: forest road; 9: main channel of Ubaye river; 10: limits of the DB landslide area.

Fig. 8 – ***Cartes des périodes de retour du glissement des Davids-Bas obtenues à partir des perturbations de croissance observées dans la tige (A), des perturbations de croissance observées dans la tige et des modifications anatomiques dates dans les sections racinaires (B)****. 1 : arbre échantillonné ; 2 : îlot herbacé ; 3 : escarpement principal ; 4 : coulée récente ; 5 : replat topographique ; 6 : dépôt torrentiel de l'Ubaye ; 7 : rupture de pente ; 10 : piste forestière ; 10 : chenal principal de l'Ubaye; 11 : limite du glissement de terrain des Davids-Bas.*

alone (fig. 8A) and with GD+AC data (fig. 8B). In figure 8A, the shortest return periods (30–35 yr) are identified in the central part of the landslide body and at altitudes comprised between 1220 and 1250 m a.s.l. Conversely, the least affected compartment of the landslide body (with return periods > 50 yr) is restricted to its westernmost part upslope to SC1. The inclusion of AC data to the return period map (fig. 8B) does not modify the global pattern of return periods but enhances the delineation of the most active compartments of the landslide body. For instance, main changes were observed in the central part of the landslide body where return periods decrease from 30–35 yr to 20–25 yr and along SC1 with a punctual decrease of up to 15 yr.

Discussion

This study reports the combined application of growth-ring signals in tree stems and exposed roots to (i) document time series of landslide reactivations in the French Alps and to (ii) identify differences in activity between several segments of the Davids-Bas landslide body. Coupled analysis of anatomical changes in 20 exposed roots and the dating of growth disturbances in 48 stems allowed documentation and mapping of 7 reactivations phases at Davids-Bas between 1977 and 2004.

At the landslide scale, synchronous responses in tree and exposed root rings confirm that exposed root samples are an efficient biological indicator for the reconstruction of rapid and abrupt events, such as landslide events. Signals resulting from root exposure observed at the DB landslide include abrupt changes in cell lumina comparable to those previously observed in torrential and river environments for instance in Poland, Czech Republic or Switzerland (*e.g.*, Malik, 2006; Hitz *et al*., 2008a,b; Malik and Matyja, 2008).

However, root-based reconstruction remains somewhat hampered by natural and methodological limitations. The key limitations of root-ring analysis of landslide activity are related (i) to the presence of trees in the study area and (ii) to the age of roots available for analysis, which does not normally exceed more than some decades. Indeed, as roots will continue to form rings and survive as long as their tips are not exposed (Schulman, 1945), roots growing adjacent to scarps are unlikely to produce as long time series as their parent trees. Datable evidence of reactivation also tends to disappear with time through complete root exposure and death, and datable evidence from root-ring records might thus be limited to more recent events. In this context, the long reconstruction presented by V.C. LaMarche (1961, 1963, 1968), P.E. Carrara and T.R. Carroll (1979) or more recently by J.R. McAuliffe *et al*. (2006) are clearly exceptional and limited to the unique environment and particular distribution of tree species in the Western United States. The cross-dating of roots has proven impossible so far, even between roots of the same tree (Krause and Eckstein, 1993;

Krause and Morin, 1999), and dead material cannot therefore be used for analysis. The restriction of analysis to living trees again limits the length of the reconstruction. The destructive sampling strategy (iii) requested for anatomical analysis of roots is another possible caveat which needs to be taken into account in the field, during analysis and from the perspective to potential monitoring, particularly in fragile and vulnerable protection forests. In addition, (iv) only one exposure signal will usually be observed in one root section, and root-ring records may not therefore produce quantitative information on return periods. Finally, (v) the reconstruction is limited to shallow landslides and to events powerful enough to damage trees (Carrara and O'Neill, 2003). It does not permit to estimate neither the rates of displacement nor the magnitude of the events.

Despite these limitations, exposed root samples allowed identification of precursor signals or initial stages of landsliding and clearly added to the analysis of reactivation phases. Coupling exposed root with stem data yields, as suggested by L. Astrade *et al*. (2012) and M. Stoffel *et al*. (2013b), very accurate information on the initiation of instability at the tree scale. They might thus provide information on the duration and magnitude of the event which could not be retrieved from stem samples alone. The coupling of growth disturbances in stem and anatomical changes in exposed roots also facilitates micro-geomorphic analyses of landslide activity, as shown, by way of example, with tree 2, located on SC1. This tree showed initial AC in 1996 in exposed root 2A (fig. 8 and fig. 9A) in the form of a sudden decrease of cell lumen area of earlywood tracheids. The reaction can be attributed clearly to an abrupt retreat of SC1 that was, however, not of sufficient intensity to tilt the tree itself, probably due to the distance of the trunk with respect to the scarp. By contrast, GD and AC were observed in the stem and in exposed roots 2B in 2001, a stretched root located perpendicularly to a tension crack upslope of SC1, and in exposed root 2C located again on SC1 (fig. 8 and fig. 9B). These reactions point to a retreat of SC1 resulting in the tilting of the stem, the exposure of exposed root 2C and the widening of the tension crack. In addition, the lateral extension of the root system allows deriving a multi-point identification of affected areas from each tree and thus an assessment of spatial coverage of the reconstruction. In that sense, exposed root-ring records sampled from the Davids-Bas landslide were particularly effective in the detection of sudden opening of cracks on the landslide body and the initiation of instability at the scarps. In addition, they have been shown in this contribution to record reactivations within specific compartments of the landslide body (cracks, scarp) for which the dendrogeomorphic record sampled from stems did not point to any activity. In that sense, and even if they do not permit detection of additional reactivation phases, exposed roots clearly contain valuable movement precursor signals at the local scale (Stoffel *et al*., 2013b) and in particular at sites with tension cracks, as the latter have been shown to be of particular interest for understanding landslide kinematics (Angeli *et al*., 2000). Tension crack opening has been monitored frequently with extensometers (Reid *et al*., 2008), GPS or automatic digital cameras (Nishii and Matsuoka, 2010) in the past, and we are convinced that the

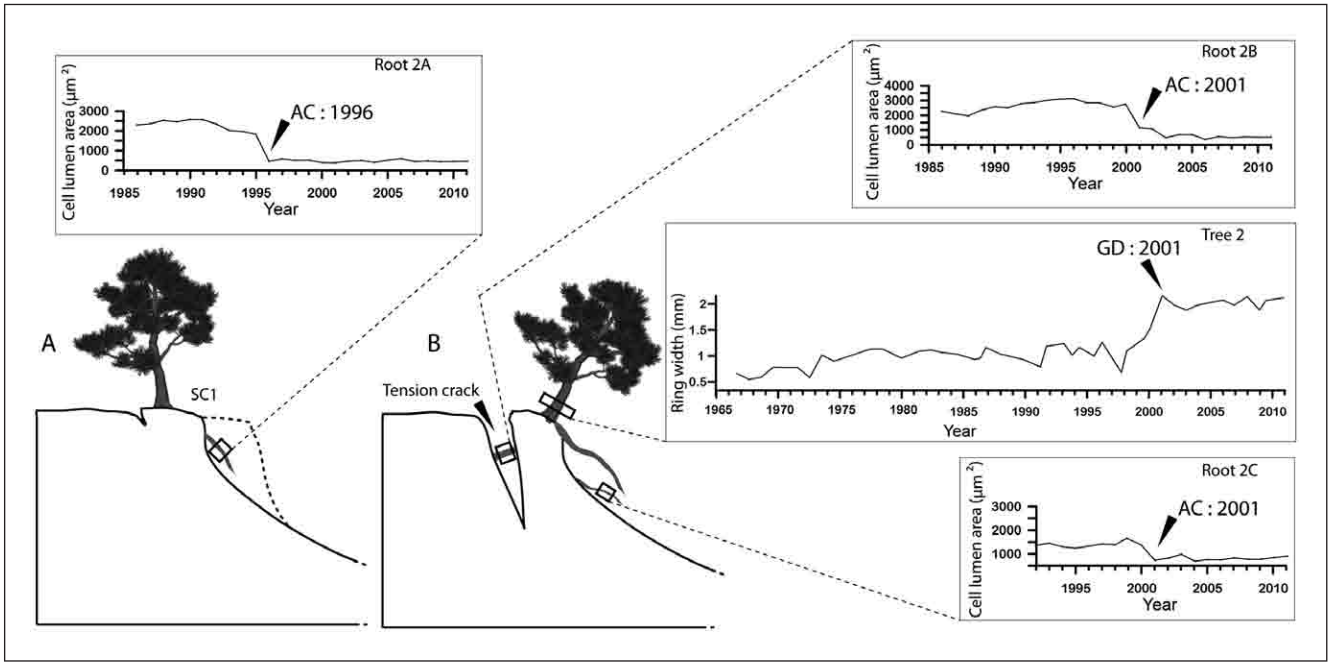

Fig. 9 – **Schematic reconstructed evolution of the main scarp (SC1) based on GD and ACs dated in tree 2.** A: scarp retreat in 1996. B: scarp retreat and crack widening in 2001.

*Fig. 9 – **Reconstitution schématique de l'évolution de l'escarpement principal basée sur les perturbations de croissance (GD) et les changements anatomiques datés dans l'arbre 2.** A : recul de l'escarpement en 1996. B : recul de l'escarpement et élargissement des fissures en 2001.*

systematic sampling of several sections of exposed roots growing perpendicular to the cracks will allow quantification of crack widening rates and their evolution (in terms of landslide pulses and/or the detection of the most unstable areas) over decadal time periods and on slopes which have remained undocumented in the past.

Conclusion

This paper reports on the coupled analysis of past movements of the Davids-Bas landslide using increment cores from affected trees and cross-sections of exposed roots being exposed by the opening of cracks. In the past, exposed root analysis was mainly used for a quantitative analysis of continuous and areal erosion processes and for the reconstruction of abrupt and severe erosion pulses resulting from gullying or torrential activity. In this study, we demonstrate that past movements can be analysed with exposed tree root samples as well and that results will not differ significantly from data obtained with classical dendrogeomorphic analysis. However, the addition of exposed roots may help significantly to improve (i) frequency maps in previously undocumented sectors of the landslide system (scars, cracks), (ii) the magnitude and duration of the event and to characterize (iii) the geomorphic evolution at the local scale.

References

Aleotti P., Chowdhury R. (1999) – Landslide hazard assessment: summary review and new perspectives. *Bulletin of Engineering Geology and the Environment* 58,1, 21-44.

Alestalo J. (1971) – Dendrochronological interpretation of geomorphic processes. *Fennia* 105, 1-139.

Amiot A., Nexon C. (1995) – *Inventaire des aléas dans le Bassin de Barcelonnette depuis 1850*. Mémoire de Maîtrise de Géographie Physique, université Louis Pasteur, Strasbourg, 173 p.

Angeli M.G., Pasuto A., Silvano S. (2000) – A critical review of landslide monitoring experiences. *Engineering Geology* 55, 133-147.

Antoine P. (1995) – Geological and geotechnical properties of the Terres noires in southeastern France: weathering, erosion, solid transport and instability. *Engineering Geology* 40, 223-234.

Antonova G.F., Stasova V.V. (1993) – Effects of environmental factors on wood formation in Scots pine stems. *Trees* 7, 214-219.

Arbellay E., Fonti P., Stoffel M. (2012) – Duration and extension of anatomical changes in wood structure after cambial injury. *Journal of Experimental Botany* 63, 3271-3277.

Astrade L., Stoffel M., Corona C., Lopez-Saez J. (2012) – L'utilisation des cernes de croissance des arbres pour l'étude des événements et des changements morphologiques : intérêts, méthodes et apports des recherches alpines à la dendrogéomorphologie. *Géomorphologie : relief, processus, environnement*, 3, 295-316.

Ballesteros-Cánovas J.A., Bodoque J.M., Lucía A., Martín-Duque J.F., Díez-Herrero A., Ruiz-Villanueva V., Rubiales J.M., Génova M. (2013) - Dendrogeomorphology in badlands: methods, case studies and prospects. *Catena* 106, 113-122.

Bégin Y., Langlais D., Cournoyer L. (1991) – Tree-ring dating of shore erosion events (Upper St Lawrence stream, eastern Canada). *Geografiska Annaler* 73A, 53-59.

Bodoque J.M., Díez-Herrero A., Martín-Duque J.F., Rubiales J.M., Godfrey A., Pedraza J., Carrasco R.M., Sanz M.A. (2005) – Sheet erosion rates determined by using dendrogeomorphological analysis of exposed tree roots: two examples from Central Spain. *Catena* 64, 81-102.

Bodoque J.M., Lucía A., Ballesteros J.A., Martín-Duque J.F., Rubiales J.M., Genova M. (2011) – Measuring medium-term sheet erosion in gullies from trees: A case study using dendrogeomorphological analysis 636 of exposed pine roots in central Iberia. *Geomorphology* 134, 417-425.

Bollati I., Della Seta M., Pelfini M., Del Monte M., Fredi P., Palmieri E. (2012) – Dendrochronological and geomorphological investigations to assess water erosion and mass wasting processes in the Apennines of Southern Tuscany (Italy). *Catena* 90, 1-17.

Bollschweiler M., Stoffel M., Schneuwly D. (2008) – Dynamics in debris-flow activity on a forested cone a case study using different dendroecological approaches. *Catena* 72, 67-78.

Boudreau S., Payette S., Morneau C., Couturier S. (2003) – George River caribou herdas revealed by tree-ring analysis. *Arctic, Antarctic, and Alpine Research* 35, 187-195.

Bräker O. (2002) – Measuring and data processing in tree-ring research? A methodological introduction. *Dendrochronologia* 20, 203-216.

Butler D.R., Malanson G.P. (1985) – A history of high-magnitude snow avalanches, southern Glacier National Park, Montana, U.S.A. *Mountain Research and Development* 5, 175-182.

Carrara P.E., Carroll T.R. (1979) – The determination of erosion rates from exposed tree roots in the Piceance Basin, Colorado. *Earth Surface Processes and Landforms* 4, 307-317.

Carrara P., O'Neill J.M. (2003) – Tree-ring dated landslide movements and their relationship to seismic events in southwestern Montana, USA. *Quaternary Research* 59, 25-35.

Chartier M.-P., Rostagno C.M., Roig F.A. (2009) – Soil erosion rates in rangelands of northeastern Patagonia: A dendrogeomorphological analysis using exposed shrub roots. *Geomorphology* 106, 344-351.

Cook E., Kairiukstis L. (1990) – *Methods of Dendrochronology: Applications in the Environmental Science*. Kluwer Academic Publishers, International Institute for Applied Systems Analysis, Dordrecht, Netherlands.

Corona C., Rovéra G., Lopez Saez J., Stoffel M., Perfettini P. (2010) – Spatio-temporal reconstruction of snow avalanche activity using tree rings: Pierres Jean Jeanne avalanche talus, massif de l'Oisans, France. *Catena* 83, 107-118.

Corona C., Lopez Saez J., Rovéra G., Astrade L., Stoffel M., Berger F. (2011a) – Quantification des vitesses d'érosion au moyen de racines déchaussées: validation de la méthode dans les badlands marneux des bassins versants expérimentaux de Draix (Alpes de Haute-Provence). *Géomorphologie : relief, processus, environment*, 11, 83-94.

Corona, C., Lopez Saez J., Rovera G., Stoffel M., Astrade L., Berger F. (2011b) – High resolution, quantitative reconstruction of erosion rates based on anatomical changes in exposed roots at Draix, Alpes de Haute-Provence — critical review of existing approaches and independent quality control of results. *Geomorphology* 125, 433-444.

Danzer S.R. (1996) – Rates of slope erosion determined from exposed roots of ponderosa pine at Rose Canyon Lake, Arizona.

In Dean, J., Meko, D.M., Swetnam, T.W. (Eds.) *Tree Rings, Environment, and Humanity*. University of Arizona, Tucson, 671-678.

Den Ouden J., Sass-Klaassen U.G.W., Copini P. (2007) – Dendrogeomorphology – a new tool to study drift-sand dynamics. *Netherlands Journal of Geosciences – Geologie en Mijnbouw* 86, 355-363.

Dubé S., Filion L., Hétu B. (2004) – Tree-ring reconstruction of high-magnitude snow avalanches in the northern Gaspé Peninsula, Québec, Canada. *Arctic, Antarctic, and Alpine Research* 36, 555-564.

Dunne T., Dietrich W.E., Brunengo J. (1978) – Recent and past erosion rates in semi-arid Kenya. *Zeitschrift für Geomorphologie* 29, 130-140.

Fantucci R. (2007) – Dendrogeomorphological analysis of shore erosion along Bolsena lake (Central Italy). *Dendrochronologia* 24, 69-78.

Flageollet J.-C. (1999) – Landslides and climatic conditions in the Barcelonnette and Vars basins (Southern French Alps, France). *Geomorphology* 30, 65-78.

Gärtner H., Schweingruber F.H., Dikau R. (2001) – Determination of erosion rates by analyzing structural changes in the growth pattern of exposed roots. *Dendrochronologia* 19, 81-91.

Gärtner H. (2007) – Tree roots: methodological review and new development in dating and quantifying erosive processes. *Geomorphology* 86, 243-251.

Guzzetti F. (2000) – Landslide fatalities and the evaluation of landslide risk in Italy. *Engineering Geology* 58, 89-107.

Hilker N., Badoux A., Hegg C. (2009) – The Swiss flood and landslide damage database 279 1972–2007. *Natural Hazards and Earth System Science* 9, 913-925.

Hitz O.M., Gärtner H., Heinrich I., Monbaron M. (2008a) – Application of ash (*Fraxinus excelsior* L.) roots to determine erosion rates in mountain torrents. *Catena* 72, 248-258.

Hitz O.M., Gärtner H., Heinrich I., Monbaron M. (2008b) – Wood anatomical changes in roots of European ash (*Fraxinus excelsior* L.) after exposure. *Dendrochronologia* 25, 145-152.

Koprowski M., Winchester V., Zielski A. (2010) – Tree reactions and dune movements: Slowinski National Park, Poland. *Catena* 81, 55-65.

Krause C., Eckstein D. (1993) – Dendrochronology of roots. *Dendrochronologia* 11, 9-23.

Krause C., Morin H. (1999) – Root growth and absent rings in mature black spruce and balsam fir, Quebec, Canada. *Dendrochronologia*, 16/17, 21-35.

LaMarche V.C. (1961) – Rate of slope erosion in the White Mountains, California. *Geological Society of America Bulletin* 72, 1579-1580.

LaMarche V.C. (1963) – Origin and geologic significance of buttress roots of bristlecone pines, White Mountains, California. *U.S. Geological Survey Professional Paper* 475-C, 149-150.

LaMarche V.C. (1968) – Rates of slope degradation as determined from botanical evidence, White Mountains, California. *U.S. Geological Survey Professional Paper* 352-I, 341-377.

Lopez Saez J. (2011) – *Reconstruction de l'activité des glissements de terrain au moyen d'une approche dendrogéomorphologique (Moyenne vallée de l'Ubaye, Alpes de Haute Provence, France)*. Thèse de doctorat, Université Grenoble, 374 p.

Lopez Saez J., Corona C., Stoffel M., Schoeneich P., Berger F. (2012a) – Probability maps of landslide reactivation derived from tree-ring records: Pra Bellon landslide, southern French Alps. *Geomorphology* 138, 189-202.

Lopez Saez J., Corona C., Stoffel M., Astrade L., Berger F., Malet J.-P. (2012b) – Dendrogeomorphic reconstruction of past landslide reactivation with seasonal precision: The Bois Noir landslide, southeast French Alps. *Landslides* 9, 189-203.

Lopez Saez J., Corona C., Stoffel M., Rovéra G., Astrade L., Berger F. (2011) – Mapping of erosion rates in marly badlands based on a coupling of anatomical changes in exposed roots with slope maps derived from LiDAR data. *Earth Surface Processes and Landforms* 36, 1162-1171.

Luo M., Zhou Y., Wang K.K. (2011) – Response of anatomical features of broadleaf tree root in Karst area to soil erosion. *Procedia Engineering* 18, 232-239.

Magliulo P., Di Lisio A., Russo F., Zelano A. (2008) – Geomorphology and landslide susceptibility assessment using GIS and bivariate statistics: a case study in southern Italy. *Natural Hazards* 47, 411-435.

Malik I. (2006) – Gully erosion dating by means of anatomical changes in exposed roots (Proboszczowicka Plateau, Southern Poland). *Geochronometria* 25, 57-66.

Malik I. (2008) – Dating of small gully formation and establishing erosion rates in old gullies under forest by means of anatomical changes in exposed tree roots (southern Poland). *Geomorphology* 93, 421-436.

Malik I., Matyja M. (2008) – Bank erosion history of a mountain stream determined by means of anatomical changes in exposed tree roots over the last 100 years (Bila Opava River - Czech Republic). *Geomorphology* 98, 126-142.

Mattheck C. (1993) – Design in der Natur. Rom bach Wissenschaft. *Reihe Okologie* 1, 242.

McAuliffe J.R., Scuderi L.A., McFadden L.D. (2006) – Tree-ring record of hillslope erosion and valley floor dynamics: Landscape responses to climate variation during the last 400 yr in the Colorado Plateau, north eastern Arizona. *Global and Planetary Change* 50, 184-201.

McCord V.A.S. (1987) – *Late Holocene sediment yield and transport in a northern Arizona drainage basin reconstructed by tree-ring analysis*. U.S. Department of Energy, Publication CONF-8608144, 213-223.

McClung D., Schaerer P. (1993) – *The Avalanche Handbook*. Mountaineers, Seattle, WA.

Nishii R., Matsuoka N. (2010) – Monitoring rapid head scarp movement in an alpine rockslide. *Engineering Geology* 115, 49-57.

Panshin A., De Zeeuw C. (1970) – *Textbook of Wood Technology*, 3e éd., McGraw-Hill, New York, USA.

Pelfini M., Santilli M. (2006) – Dendrogeomorphological analyses on exposed roots along two mountain hiking trails in the Central Italian Alps. *Geografiska Annaler* 88A, 223-236.

Pérez-Rodríguez R., Marques M.J., Bienes R. (2007) – Use of dendrochronological method in *Pinus halepensis* to estimate the soil erosion in the South East of Madrid (Spain). *Science of the Total Environment* 378, 156-160.

Petrascheck A., Kienholz H. (2003) – Hazard assessment and mapping of mountain risks in Switzerland. *In* Rickenmann D., Chen C.L. (Eds.) *Debris Flow Hazards Mitigation: Mechanics,*

Prediction and Assessment. Millpress, Rotterdam, Netherlands, 25-38.

Reardon B.A., Pederson G.T., Caruso C.J., Fagre D.B. (2008) – Spatial reconstructions and comparisons of historic snow avalanche frequency and extent using tree rings in Glacier National Park, Montana, U.S.A. *Arctic, Antarctic, and Alpine Research* 40, 148-160.

Reid M., Baum R., LaHusen R., Ellis W. (2008) – Capturing landslide dynamics and hydrologic triggers using near-real-time monitoring. *In* Chen, Z., Zhang, J., Li, Z., Wu, F., Ho, K. (Eds.) *Landslides and Engineered Slopes. From the Past to the Future*. CRC Press, 179-191.

Rovéra G., Lopez Saez J., Corona C., Stoffel M., Berger F. (2013) – Preliminary quantification of the erosion of sandy-gravelly cliffs on the island of Porquerolles (Provence, France) through dendrogeomorphology, using exposed roots of Aleppo pine (*Pinus halepensis* Mill.). *Geografia Fisica e Dinamica Quaternaria* 36, 181-187.

Rubiales J.M., Bodoque J.M., Ballesteros J.A., Díez A. (2008) – Response of *Pinus sylvestris* roots to sheet-erosion exposure: an anatomical approach. *Natural Hazards and Earth System Sciences* 8, 223-231.

Schulman E. (1945) – Root growth-rings and chronology. *Tree-Ring Bulletin* 12, 2-5.

Schweingruber F.H. (1996) – *Tree rings and environment, Dendroecology*. Paul Haupt, Bern, Stuttgart, Wien, 609 p.

Shewbridge S.E., Sitar N. (1989) – Deformation characteristics of reinforced sand in direct shear. *Journal of Geotechnical Engineering* 115, 1134-1147.

Shroder J. (1978) – Dendrogeomorphological analysis of mass movement on Table Cliffs Plateau, Utah. *Quaternary Research* 9, 168-185.

Skaugset A. (1997) – *Modeling root reinforcement in shallow forest soils*. Ph.D. thesis, Oregon State University, Corvallis, Oreg., 456 p.

Silhan K. (2012) – Dendrogeomorphological analysis of the evolution of slope processes on Flysch rocks (Vsetinske Vrchy Mts, Czech Republic). *Carpathian Journal of Earth and Environmental Sciences* 7, 39-49.

Stefanini M. (2004) – Spatio-temporal analysis of a complex landslide in the northern Apennines (Italy) by means of dendrochronology. *Geomorphology* 63, 191-202.

Stoffel M, Schneuwly D., Bollschweiler M., Lievre I., Delaloye R., Myint M., Monbaron M. (2005) – Analyzing rockfall activity (1600–2002) in a protection forest — a case study using dendrogeomorphology. *Geomorphology* 68, 224-241.

Stoffel M., Perret S. (2006) – Reconstructing past rockfall activity with tree rings: some methodological considerations. *Dendrochronologia* 24, 1-15.

Stoffel M., Bollschweiler M. (2008) – Tree-ring analysis in natural hazards research — an overview. *Natural Hazards and Earth System Science* 8, 187-202.

Stoffel M., Bollschweiler M., Butler D.R., Luckman B. (2010) – *Tree Rings and Natural Hazards*. Springer, Dordrecht, New York.

Stoffel M., Casteller A., Luckman B.H., Villalba R. (2012) – Spatiotemporal analysis of channel wall erosion in ephemeral torrents using tree roots — an example from the Patagonian Andes. *Geology* 40, 247-250.

Stoffel M., Butler D., Corona C. (2013a) – Mass movements and tree rings: A guide to dendrogeomorphic field sampling and dating. *Geomorphology* 200, 106-120.

Stoffel M., Corona C., Ballesteros-Cánovas J.A., Bodoque J.M. (2013b) – Dating and quantification of erosion processes based on exposed roots. *Earth-Science Reviews* 123, 18-34.

Stokes M.A., Smiley T.L. (1968) – *An introduction to tree-ring dating*. University of Chicago Press, Chicago, 73 p.

Thiery Y., Malet J.-P., Sterlacchini S., Puissant A., Maquaire O. (2007) – Landslide susceptibility assessment by bivariate methods at large scales: application to a complex mountainous environment. *Geomorphology* 92, 38-59.

Timell T. (1986) – *Compression Wood in Gymnosperms*. Springer-Verlag, Berlin, New York.

Van Den Eeckhaut M., Muys B., Van Loy K., Poesen J., Beeckman H. (2009) – Evidence for repeated re-activation of old landslides under forest. *Earth Surface Processes and Landforms* 34, 352-365.

Vandekerckhove L., Muys B., Poesen J., De Weerdt B., Coppé N. (2001) – A method for dendrochronological assessment of medium-term gully erosion rates. *Catena* 45, 123-161.

Zimmermann M.H. (1983) – *Xylem Structure and the Ascent of Sap*. Springer Verlag, New-York, 143 p.

Article soumis le 10 juillet 2013, accepté le 6 février 2014.